 doi:10.20944/preprints202207.0065.v1

Article

The Bovine Seminal Plasma Protein PDC-109 Possesses Pan-Antiviral Activity

Hannah Sabeth Schwarzer-Sperber[1], Kathrin Sutter[1,2], Karin Müller[3], Peter Müller[4*] and Roland Schwarzer[1,*]

[1] University Hospital Essen, Institute for Translational HIV Research, Hufelandstraße 55, 45147 Essen, Germany, https://www.uni-due.de/hiv/ag_schwarzer/navigation.php, + 49 (0) 201-723-4343 (not to be published), Roland-Schwarzer@gmx.de,
[2] University Hospital Essen, Institute for Virology, Virchowstr. 171, 45147 Essen, Germany
[3] Leibniz Institute for Zoo and Wildlife Research, Alfred-Kowalke-Straße 17, 10315 Berlin, Germany
[4] Humboldt-University Berlin, Department of Biology, Invalidenstr. 42, 10115 Berlin, Germany, +49-30-2093-98463 (not to be published), peter.mueller.3@rz.hu-berlin.de

Abstract

Mammalian seminal plasma contains a multitude of bioactive components, including lipids, glucose, mineral elements, metabolites, proteins, cytokines and growth factors, with various functions during insemination and fertilization. The seminal plasma protein PDC-109 is one of the major soluble components of the bovine ejaculate and is crucially important for sperm motility, capacitation and acrosome reaction. A hitherto underappreciated function of seminal plasma is its anti-microbial and anti-viral activity, which may limit sexual transmission of infectious diseases during intercourse. We have recently discovered that PDC-109 inhibits the membrane fusion activity of influenza virus particles and significantly impairs viral infections at micromolar concentrations. Here we investigated whether the antiviral activity of PDC-109 is restricted to Influenza or if other mammalian viruses are similarly affected. We focused on Severe Acute Respiratory Syndrome Coronavirus-2 (SARS-CoV-2), the etiological agent of the Coronavirus Disease 19 (COVID-19), thoroughly assessing PDC-109 inhibition with SARS-CoV-2 Spike (S)-pseudotyped reporter virus particles, but also live-virus infections. Consistent with our previous publications we found significant virus inhibition, albeit accompanied by substantial cytotoxicity. Using time-of-addition experiments however, we discovered treatment regimen that enable virus suppression without affecting cell viability. We furthermore demonstrated that PDC-109 is also able to impair infections mediated by the VSV glycoprotein (VSVg) thus indicating a broad pan-antiviral activity against multiple virus species and families.

Keywords: SARS-CoV-2; VSV replicon; PDC-109; Bovine seminal plasma; Fn-type 2 proteins

Introduction

One major route of infection for both viral and bacterial pathogens is sexual contact. Infections can induce an insurmountable number of sexually transmitted diseases (STD) causing severe, often life-threatening pathologies and large-scale epidemics within human populations.. The abundance of viruses in male ejaculates and seminal plasma has severe consequences for the male and, after sexual transmission, the recipient sexual partner [1] and it is reasonable to assume that hosts have evolved

 doi:10.20944/preprints202207.0065.v1

ample mechanisms to cope with this threat. In search of novel antiviral substances, we have focused our present study on mammalian seminal plasma (SP), which has been previously shown to possess antiviral activities [2,3]. Interestingly, SP contains both pro- and antiviral agents, amongst them differently acting hormones, cytokines and growth factors. Virus infection promoting factors include amyloid fibrils [4] (which are aggregated fragments of the prostatic acid phosphatase), substances neutralizing the vaginal acidic pH [5], and complement fragments enhancing virus–target cell attachment [6]. In contrast, proteins such as defensins, lactoferrin, and clusterin exert antiviral activity which is likely to protect spermatozoa against viral contaminations within the male and female genital tract [7,8]. Moreover, human seminal exosomes have been shown to possess anti-HIV-1 activity [9–13].

Recently, we have found that the SP protein PDC-109 (also known as BSP-1/2) is able to inhibit the infectivity of influenza virus [14]. PDC-109 is the major component of bovine SP and belongs to a protein family containing the fibronectin type II domain (Fn II). Fn II proteins were found in SP of many other mammalian species including humans [15]. A couple of previous studies have characterized the protein, its molecular interactions, and its physiological activities/role in detail [15–20]. Briefly, PDC-109 specifically interacts with choline-containing phospholipids of (sperm) membranes and, thereby, modulates membrane and cell properties [21–24]. These alterations are part of a cascade of processes which prime the male gametes for fertilization, i.e. stabilizing sperm cells during their transit through the female genital tract, facilitating the formation of the sperm reservoir by mediating sperm-binding to the oviductal epithelium, and subsequent destabilization of the sperm membrane enabling the acrosomal exocytosis prior to fertilization [15,17,20]. Additionally, a chaperone-like activity of PDC-109 has been reported [25]. Recently, we discovered an influence of PDC-109 on influenza virus activity, which is caused by a binding of the protein to both, viral and target membranes [14]. Similar to its interaction with sperm cells, binding probably occurs to choline-containing lipids, thereby preventing virus-cell fusion. Based on this mode of action, we hypothesize that PDC-109 might exert broader antiviral effects.

To test this hypothesis, we have assessed the inhibitory activity of PDC-109 on reporter viruses, pseudotyped with either the spike protein of the severe acute respiratory syndrome coronavirus type 2 (SARS-CoV-2) or the Vesicular stomatitis virus glycoprotein (VSVg). By using two non-related virus species we sought to explore whether antiviral activity is pathogen specific or pan-viral. We observed significant, dose-dependent pan-antiviral effects of PDC-109 with only minor eukaryotic cytotoxicity upon transient administration of the protein. Interestingly, extended exposure of mammalian cells to PDC-109 lead to a marked reduction in cell viability through an unknown mechanism.

Materials and Methods

Mammalian Cell culture. The cell lines BHK-G43 (a kind gift from Gert Zimmer, Institute of Virology and Immunology, Mittelhäusern/Switzerland), Vero E6 (CRL-1586; American Type Culture Collection, Manassas, VA), Calu6 (HTB-56; American Type Culture Collection, Manassas, VA) and HEK293T (CRL-3216; American Type Culture Collection, Manassas, VA) were

 doi:10.20944/preprints202207.0065.v1

maintained in Dulbecco's modified Eagle medium (DMEM) containing 10% heat-inactivated fetal bovine serum (FBS), 2 mM L-glutamine, 100 U/ml penicillin, and 100 µg/ml streptomycin (all from PAA Laboratories GmbH, Austria) under standard cell culture conditions.

Chemicals. If not otherwise mentioned, all chemicals were purchased from Sigma-Aldrich (Taufkirchen, Germany). Phosphate buffered saline (PBS) contained 150 mM NaCl and 5.8 mM sodium phosphate (pH 7.4). HEPES buffered salt solution (HBS) contained 150 mM NaCl and 10 mM HEPES (pH 7.4).

Seminal plasma. Semen was collected from bulls (*Bos taurus taurus*) routinely used for production of doses for artificial insemination (AI) in a breeding center located in Germany. Semen production protocols were applied according to the general guidelines for semen processing used in AI centers. Semen was collected with an artificial vagina and transported to the laboratory facility within 5 min. Only aliquots of ejaculates with a sperm motility above 80% were used. Sperm cells were immediately pelleted by centrifugation (1 200 × g, 8 min, RT) and supernatant was centrifuged again in 2 ml aliquots to remove residual sperm cells (12 000 × g, 2 min, RT). SP was aliquoted and frozen (-20°C) until further processing.

Purification of PDC-109. PDC-109 was purified from delipidated SP (dSP) samples as described before [26]. Delipidation of SP was performed according to [27]. For that, SP samples were centrifuged (10 min, 10 000 g). One volume (vol) of the supernatant was mixed with 9 vol ice cold EtOH and stirred for 90 min at 4°C followed by centrifugation of the solution (10 min, 10 000 g). The resultant pellet was washed three times with ice cold EtOH (centrifugation 10 min, 10 000 g) and subsequently resolved in 1 vol 50 mM NH_4HCO_3 and finally lyophilized. The resultant powder was solved in a minimal volume of HBS followed by addition of 2 vol isopropyl ether/n-butanol (60:40) and incubation for 30 min on a shaker. The suspension was centrifuged (2 min, 1 000 g) and the organic phase containing lipids was removed by aspiration. The residual organic solvent above the water phase was eliminated by passing a gentle stream of nitrogen over the aqueous layer. The final aqueous solution containing delipidated proteins was lyophilized.

For purification of PDC-109, the freeze-dried sample was solubilized in TBS buffer (50 mM Tris, 1 M NaCl, 5 mM EDTA, pH 6.4) and centrifuged (5 min, 500 g). The supernatant was given on a DEAE A25 column (Merck KGaA, Darmstadt, Germany) linked to a Bio-Rad Econo system (Bio-Rad, Feldkirchen, Germany) and flushed with TBS until protein absorption at 280 nm declined to base line. Subsequently, PDC-109 was eluted with TBS additionally containing 100 mM choline chlorid. The fractions containing the protein were combined and extensively dialyzed against 50 mM NH_4HCO_3, pH 8.0 using dialysis tubes MEMBRA-CEL®, MW 7000 (Serva, Heidelberg, Germany) followed by lyophilization. For the experiments, PDC-109 was diluted in HBS verifying protein concentration by measuring its absorption at 280 nm (using A_{280} of 1 mg/ml = 2.5) [26].

Preprints (www.preprints.org) | NOT PEER-REVIEWED | Posted: 5 July 2022 doi:10.20944/preprints202207.0065.v1

Establishment of HEK293T and Calu6 cells stably expressing ACE2 and TMPRSS2. Human ACE2 was cloned into pLKO5d.SFFV.dCas9-KRAB.P2A.BSD (Addgene, Cat.#90332, a gift from Dirk Heckl) and TMPRSS2 was cloned into pDUAL CLDN (GFP) (Addgene, Cat.#86981, a gift from Joe Grove). Clonings were confirmed by Sanger sequencing. Lentiviral particles for delivery of lentiviral ACE2 and TMPRSS2 vectors were produced in HEK293T cells using transfection with PEI. Briefly, cells were triple transfected with the lentiviral ACE2 or TMPRSS2 constructs, psPAX2 (Addgene, Cat.#12260, a gift from Didier Trono), and pVSV-G (Addgene, Cat.# #138479, a gift from Akitsu Hotta). 48 h post transfection, cell supernatants containing the newly produced viral particles were centrifuged, filtered using 0.22 µm vacuum filter units (Merck Millipore, Darmstadt, Germany) and stored at -80°C. To establish stable cell lines, HEK293T or Calu6 cells were first transduced with lentiviral particles containing the ACE2 vector. 48 hours post transduction, medium was replaced with blastidicin (BSD; InvivoGen, San Diego, USA) selection medium. For double transduced cells, after sufficient selection and expansion of transgenic cells, another round of transduction with TMPRSS2 lentiviral particles followed. Double transduced cells were selected in antibiotic selection medium containing BSD and Puromycin 48h post transduction. The expression of ACE2 and TMPRSS2 was confirmed by Western Blot.

VSV*ΔG-fLuc pseudotyping and transduction experiments. Preparation of VSV pseudotyping has been described previously (Berger Rentsch and Zimmer, 2011). Briefly, Hek293T cells were transfected using polyethylenimine (PEI) with a SARS-CoV-2 Spike encoding plasmid (pCG1-SARS-CoV-2-Spike, kindly provided by Dr. Graham Simmons, Vitalant Research Institut) for 24 hours and subsequently infected with a single-round VSV reporter replicon (VSV*ΔG-fLuc, kindly provided by Gert Zimmer, Institute of Virology and Immunology, Mittelhäusern/ Switzerland), in which the VSVg open reading frame was replaced with an enhanced green fluorescent protein (eGFP) and a firefly luciferase.

Cell were incubated for 4 hours with the input virus at 37 °C, 5% CO_2, then washed with PBS before medium supplemented with anti-VSV-G antibody from Vi-10 hybridoma cells [28] was added in order to neutralize seed virus residues. The next day, supernatants, containing pseudotyped virus particles were harvested, cleared from cellular debris by centrifugation, filtered using Syringe Filter (0.22 µm, Sartorius, Goettingen, Germany) and stored at -80 °C.

VSV*ΔG-fLuc VSVg seed virus propagation was conducted in BHK-G43 cells as described previously (10.1099/vir.0.023978-0). Cells were pre-plated and VSVg expression was induced with 1 nM Mifepristone (Calbiochem, Darmstadt, Germany) for 6 hours at 37 °C, 5% CO_2, followed by infections with VSV*ΔG-fLuc VSVg (MOI~1) for 16-24 hours at 37 °C, 5% CO_2. Ultimately, supernatants were harvested, cleared from cellular debris by centrifugation, filtered using Syringe Filter (0.22 µm, Sartorius, Göttingen, Germany) and stored at -80 °C.

For transduction experiments, 50000 target cells were plated in 96-well flat-bottom dishes and inoculated at the next day with pseudotyped VSV*ΔG-fLuc. If not otherwise stated, cells were spin-infected for 30 min, at 1200g and 37 °C, followed by another

 doi:10.20944/preprints202207.0065.v1

90 min of incubation at 37 °C, 5% CO_2. Subsequently, virus-containing supernatant was removed and cells were further incubated for 24 hours at 37 °C, 5% CO_2. Infection levels were assessed by flow cytometry using and LSRII (Becton Dickinson, San Diego, CA, USA), equiped with a high-throughput sampling unit (HTS), gating on single, live GFP positive cells. If not otherwise stated, PDC-109 and SP was administered 15-30 min prior to and during infections. Cell viability was assessed by forward and side scatter (FSC and SSC) gating, based on gate calibration using Zombie fixable viability dyes (BioLegend, San Diego, CA, USA).

SARS-CoV-2 propagation, titration and TCID50 experiments. The SARS-CoV-2 isolate used in this study was obtained from patient material and propagated in VeroE6 cells as previously described [29]. Briefly, 2×10^6 VeroE6 cells were seeded in a T75 flask and maintained in Dulbecco's modified Eagle's medium (DMEM) supplemented with 10% fetal bovine serum (FBS), L-glutamine, penicillin, and streptomycin for 24 hours at 37 °C, 5% CO_2. Then, cells were infected with isolated virus, cultured for another 72 hours. Finally, the supernatant was harvested, cell debris was removed by centrifugation and supernatant aliquots were stored at −80 °C. Viral titers were determined by endpoint dilution assay in order to calculate the 50% tissue culture infective dose (TCID50). SARS-CoV-2 inhibition was tested by TCID50 assays using suited inoculums of virus and titrations of antiviral compounds. Cells were pre-treated for 15-30 minutes with antiviral reagents and subsequently infected in their presence for 2 hours at 37 °C, 5% CO_2. Then, virus-containing supernatants were removed and cells were incubated for another 72 hours. Finally, crystal-violet staining was performed in order to identify inhibition of viral cytopathic effects. 8-10 wells were typically assessed per drug concentration and the fraction of wells without plaques was calculated as a measure of SARS-CoV-2 infection.

SARS-CoV-2 In-Cell ELISA. Virus quantification by In-Cell ELISA was performed as recently described [30]. Briefly, 5×10^4 cells/well (flat-bottom 96-well plate) were plate one day pre-infection. Then, cells were infected with SARS-CoV-2 for 16-24 hours and fixed with 4% (w/v) paraformaldehyde/PBS. Then, 1% (v/v) Triton-X-100/PBS was used for permeabilization, followed by blocking with 3% (v/v) FCS/PBS. Subsequently, the primary antibody (anti-N mAb1 ABIN6952435, Antibodies Online, Aachen, Germany) was added and incubated for 2 h at room temperature or overnight at 4°C. Peroxidase-labelled secondary antibody (Cat.#115-035-003, Jackson Immuno Research, Cambridge, UK) was added for another 1–2 hours prior to washing steps with 0.05% (v/v) Tween-20/PBS. Finally, Tetramethylbenzidin (TMB) substrate was added and the enzymatic reaction was stopped with 0.5 M HCl. Absorbance of the dye was measured at 450 nm using a Spark 10M multimode microplate reader (Tecan, Maennedorf, Switzerland).

Statistics. If not stated otherwise, bars show arithmetric mean ± SEM. Statistical significance was assessed using Prism (GraphPad Software Inc., San Diego, CA, USA), applying parametric one-way analysis of variance (ANOVA) tests and displayed as follows: **** $p < 0.0001$; *** $p < 0.001$; ** $p = 0.001–0.01$; * $p = 0.01–0.05$. Data were tested for normality by Shapiro-Wilk test using a significance level of 0.05,

Preprints (www.preprints.org) | NOT PEER-REVIEWED | Posted: 5 July 2022 doi:10.20944/preprints202207.0065.v1

Results

We have recently demonstrated that PDC-109 possesses antiviral properties, effectively blocking influenza virus fusion with plasma membranes of susceptible red blood cells [14]. Here, we sought to test whether PDC-109 is also capable of inhibiting the activity of viruses other than influenza.

PDC-109 effectively blocks infections with SARS-CoV-2 pseudotypes. Initially, we tested if PDC-109 is able to inhibit infections with SARS-CoV-2 Spike-pseudotyped VSV* (VSV*SARS CoV-2). As cellular target we utilized Calu6 ACE2 cells, a transgenic cell line that was transduced with human angiotensin converting enzyme 2 (ACE2, Supplementary Figure S1A). Calu6 ACE2 cells stably express ACE2, the canonical receptor of SARS-CoV-2 (Figure S1B), rendering this lung epithelial cell line permissive for SARS-CoV-2 pseudotypes. The parental cell line, on the other hand, is refractive to SARS-CoV-2 infections, which enables effective testing of SARS-CoV-2 pseudotypes for ACE2 specificity (Supplementary Figure S1C). We first incubated Calu6 ACE2 cells with increasing concentrations of PDC-109 followed by an infection with VSV*SARS CoV-2 for 24 h (Figure 1A). A strong, dose-dependent inhibition of infection was found at double digit micromolar concentrations. Notably, we also observed a significant cytotoxicity of the protein at concentrations >25 µM (Figure 1A). However, by decreasing the PDC-109 administration regimen to the initial 2 h of infection, we were able to achieve significant inhibition of virus infection, with negligible cytotoxic effects (Figure 1B).

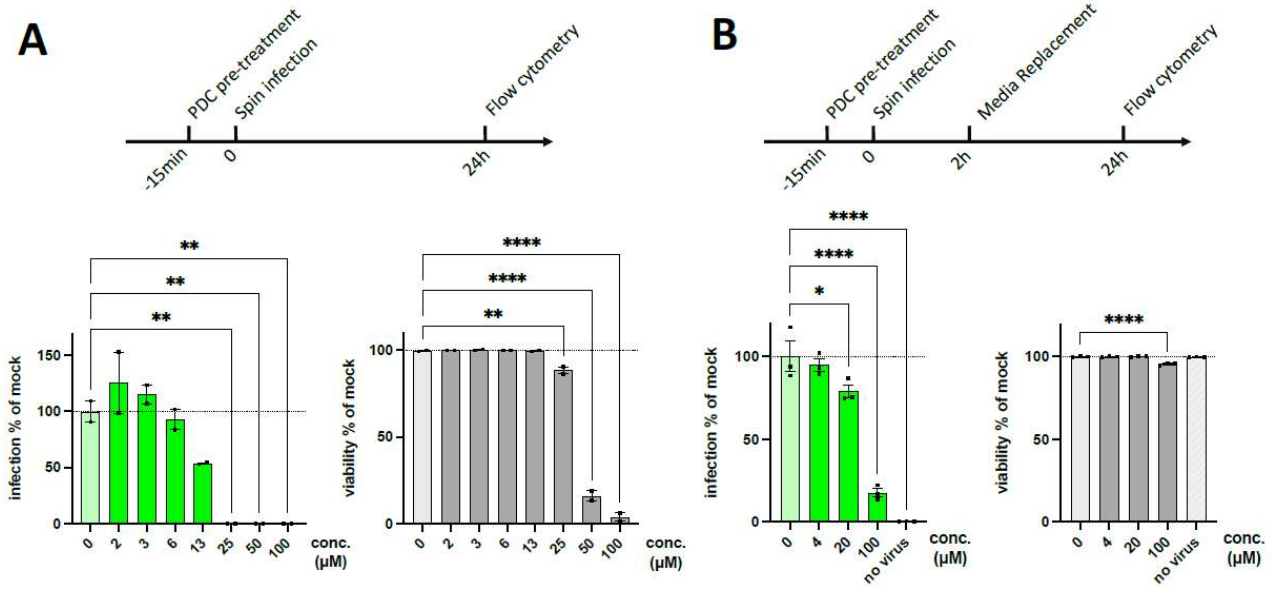

Figure 1: Anti-SARS-CoV-2 activity of PDC-109. (A) Calu6 ACE2 cells were pre-treated with different concentrations PDC-109 for 15 min and spin-infected with CoV-2 spike pseudoviruses. Then, cells were incubated with virus and PDC-109 for 24 hours. **(B)** Calu6 ACE2 cells were pre-treated with different concentrations of PDC for 15 min and spin-infected with CoV-2 spike pseudo-viruses in presence of PDC. Subsequently, excess virus and PDC were removed after 2 hours of incubation and cells were cultured for another 24 hours. Reporter virus signal and cell viability were assessed by flow cytometry. Frequencies of GFP+ cells are shown as a measure of VSV*SARS CoV-2 infection and were normalized to mock-treated samples. Significance was assesed by parametric one-way analysis of variance (ANOVA) tests, comparing all samples with the mock control (0 µM) and displayed as follows: ****P < 0.0001; ***P < 0.001; **P = 0.001–0.01; *P = 0.01–0.05.

Preprints (www.preprints.org) | NOT PEER-REVIEWED | Posted: 5 July 2022 doi:10.20944/preprints202207.0065.v1

PDC-109 interferes with SARS-CoV-2 mediated entry and reporter virus replication. The results described above indicate that PDC-109 has substantial, inhibitory effects on virus infections, mediated by SARS-CoV-2 spike proteins. Next, we investigated whether the protein also impairs other steps of viral replication cycles. For that, a series of time-of-addition experiments were performed with varying PDC-109 administration intervals (Figure 2A). Cells were exposed to the protein either (i) for the entire 24 h virus replication period, (ii) for the first 2 h of virus entry only, or (iii) 2 h after initiating virus infection. Interestingly, PDC-109 reduced infection levels in all experimental setups (Figure 2B), including post-entry administration (2-24 h). This indicates multifactorial effects of PDC-109 on both, SARS-CoV-2 mediated virus entry and VSV* dominated replication and GFP expression. Again, we observed significant toxicity throughout all PDC-109 treated samples (albeit of negligible extent for 2 h treatments), which may confound the potential, antiviral effects at longer administration periods.

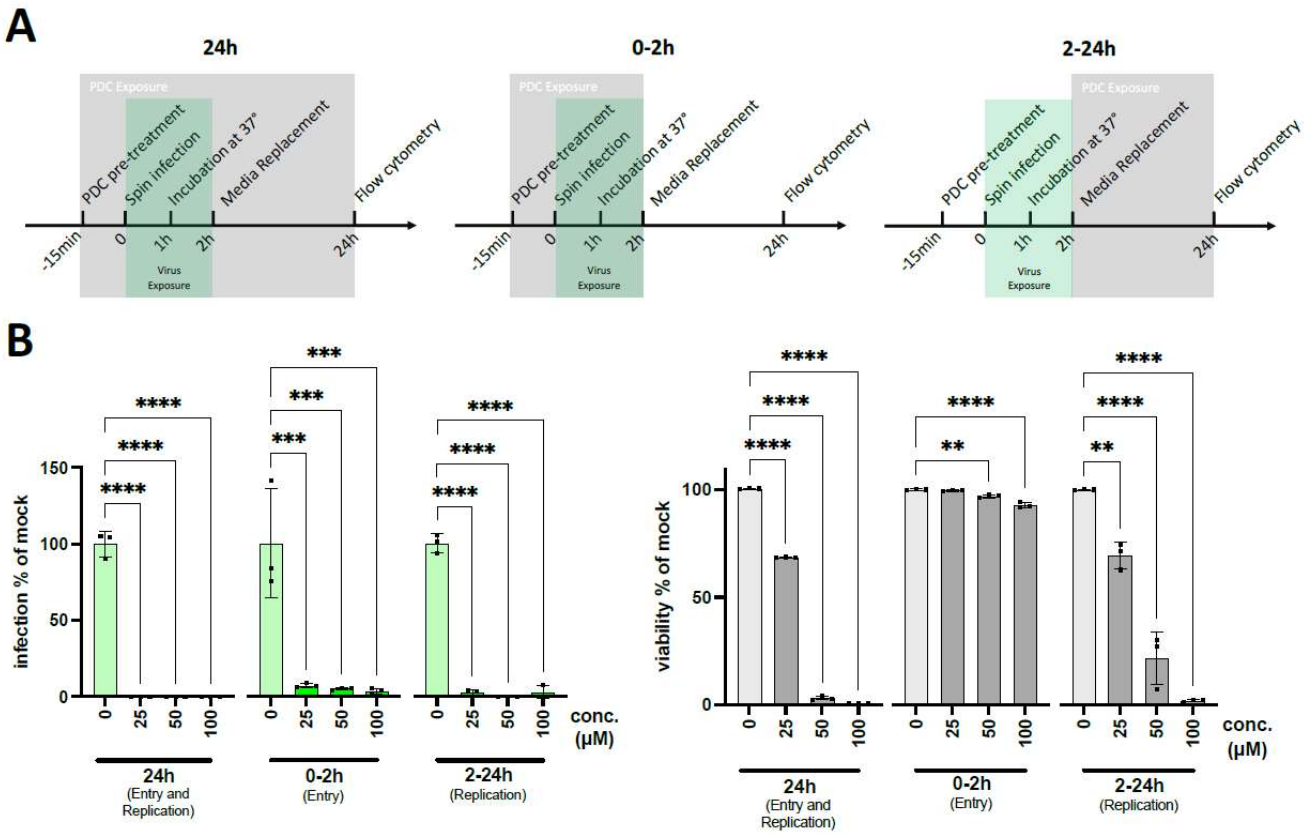

Figure 2: PDC-109 effects on virus entry and replication. **(A)** Experimental workflow for time-of-addition assay. Calu6 ACE2 cells were exposed to various concentrations of PDC at different phases of infection. 24 h samples were incubated with PDC (grey box) for the entire infection period (green box), thus blocking virus entry and reporter virus infection. 0-2 h samples were incubated with PDC for the initial 2 h of infection only, limiting direct antiviral effects predominantly to the entry stage of infection. 2-24 h samples were treated with PDC at 2 h post infection and therefore after successful viral entry**. (B)** Infection and viability were assessed by flow cytometry at 24 h post infection. Significance was assesed by parametric one-way analysis of variance (ANOVA) tests, comparing all samples with the mock control (0 µM) and displayed as follows: ****P < 0.0001; ***P < 0.001; **P = 0.001–0.01; *P = 0.01–0.05.

Preprints (www.preprints.org) | NOT PEER-REVIEWED | Posted: 5 July 2022 doi:10.20944/preprints202207.0065.v1

Cells are not protected from SARS-CoV-2 Spike-mediated entry after PDC-109 pre-treatment. PDC-109 has been shown to bind to membranes modulating the structure and dynamics of membrane lipids [21–24]. Thus, we speculated whether the impact of the protein on virus infectivity is mediated by modifications of cellular membranes. In that case, PDC-109 may induce irreversible changes that could render cellular membranes non-permissive for viral infections even after its removal from cell culture media. To test this hypothesis, we uzilized two transgenic sub-cell lines with different permissivities for SARS-CoV-2 mediated entry. Both, 293T ACE2 and 293T ACE2 TMPRSS2 were derived from 293T cells that have been transduced with ACE2 and TMPRSS2, respectively. TMPRSS2 is an entry co-factor for CoV-2 infections[31] and strongly facilitates spike-mediated membrane fusion (Figure 3A and B, see "no PDC" samples). These two cell lines were utilized in order to investigate whether only a pretreatment of cells with PDC-109 affects moderately (293T ACE2) and highly permissive (293T ACE2 TMPRSS2) cells differently. Noteworthily, neither cell line was protected from VSV*SARS CoV-2 infection upon PDC-109 priming (Figure 3A), whereas infections in presence of PDC-109 were again heavily decreased (Figure 3B). This finding indicates that PDC-109 effects on virus infectivity are transient and rapidly wane after its removal from treated cells.

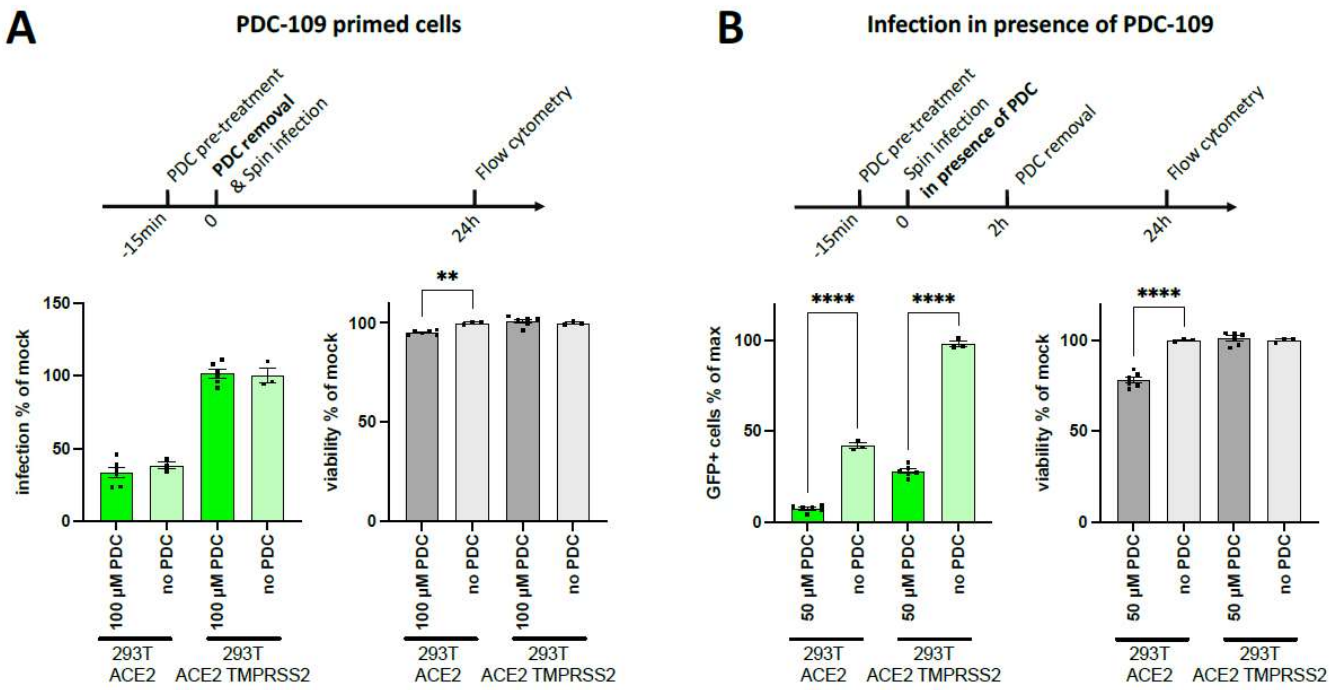

Figure 3: Permissivity of PDC-109 pre-treated cells. (A) 293T ACE2 and 293T ACE2 TMPRSS2 cells were pre-treated with 100 µM PDC-109 for 15 min and spin-infected with CoV-2 spike pseudoviruses in absence of PDC. **(B)** 293T ACE2 and 293T ACE2 TMPRSS2 cells were pre-treated with 50 µM PDC-109 for 15 min and spin-infected with CoV-2 spike pseudoviruses in presence of PDC for 30 min, followed by 90 min incubation at 37°C. Subsequently, cell were washed and cultured further. Reporter virus signal and cell viability were assessed by flow cytometry at 24 h p.i.. Significance was assesed by parametric one-way analysis of variance (ANOVA) tests, comparing all samples with their respective mock control (no PDC) and displayed as follows: ****P < 0.0001; ***P < 0.001; **P = 0.001–0.01; *P = 0.01–0.05.

PDC-109 reduces SARS-CoV-2 infection *in cellulo*. Finally, we assessed whether PDC-109 affects live SARS-CoV-2 infections in cell culture. For that, TCID50 assays were employed and the antiviral effects were determined upon 72 h of infection in the

Preprints (www.preprints.org) | NOT PEER-REVIEWED | Posted: 5 July 2022 doi:10.20944/preprints202207.0065.v1

presence of increasing concentrations of PDC-109. In agreement with our pseudovirus experiments, treated cells showed a protection from CoV-2 infections up to levels of around 50% at concentrations above 20 µM (Figure 4A). We note that in this experimental setup PDC-109 was only present during the first two hours of infection whereas spreading infections of the wildtype virus are permitted for several days. By that, secondary rounds of infections can be presumed not to be affected by the initial PDC-109 treatment. This latter limitiation strongly decreases the maximal antiviral effect to be expected, and we hypothesized that the observed decrease of infection levels is in fact indicative of a more pronounced inhibition of viral entry in the presence of PDC-109. To test this hypothesis we employed an alternative assay, an in-cell ELISA, which can detect viral proteins in infected cells already at 24 hours post infection. Our data show almost complete inhibition of viral infection at the highest PDC-109 concentration, which supports the notion that PDC-109 possesses strong

antiviral effects against SARS-CoV-2. Importantly, we did not find noticeable toxicity effects of a 2 h PDC-109 treatment in absence of viral infection (Supplementary Figure S2).

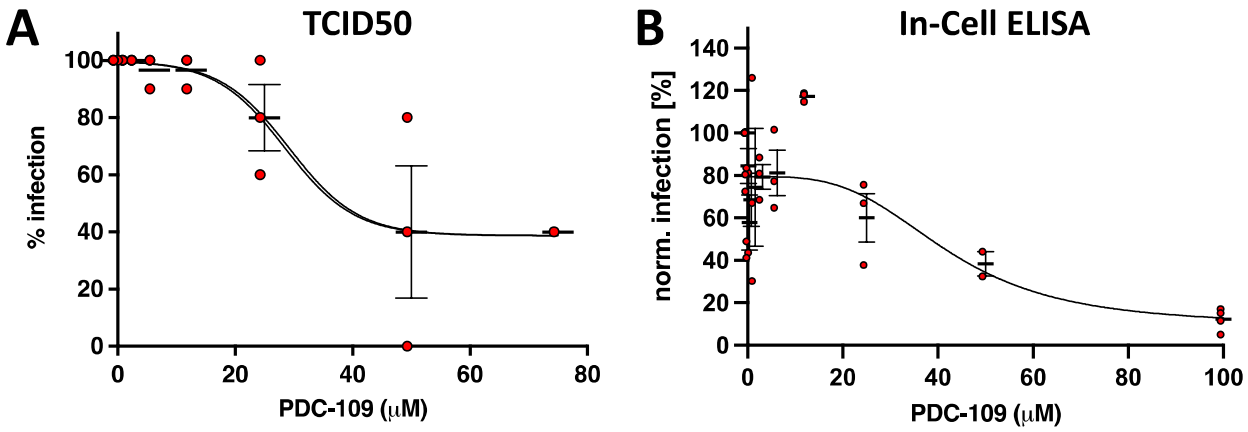

Figure 4: PDC-109 effects on live CoV-2 infection in cell culture. The antiviral activity of PDC was assessed by TCID50 assay or In-Cell ELISA. **(A)** VeroE6 cells were pre-treated with different concentrations of PDC in 10 repeats for 15 min and incubated with infectious CoV-2 (Essen isolate) for 2 hours at 37°C. Subsequently, PDC containing media were replaced with fresh media and cells were incubated for another 3 to 5 days to allow for spreading infections in the cell culture. Trypan blue staining was conducted to determine viral cytopathic effects. The frequency of wells with intact cell monolayers per PDC concentration was utilized as a measure of viral infectivity. Each point represents the data of one independent experiment. **(B)** In-Cell ELISA was performed 24 h post infection. Dots show the mean of three technical repeats per condition from 2-3 independent experiments. Thick lines show arithmetic mean with SEM. B shows data normalized to mock treated infection controls.

PDC-109 inhibits entry of VSV into VeroE6 cells.

Our previous experiments have unequivocally shown, that PDC-109 has the potential to inhibit SARS-CoV-2 Spike-mediated entry in different permissive cell lines and can even alleviate viral cytopathic effects in authentic live-virus infection assays. We now sought to investigate whether its antiviral activity is limited to Influenza [14] and SARS-CoV-2 (Figure 1-Figure *4*), or whether other virus pseudotypes would be equally blocked. Therefore, we tested VSV* seed particles, which are essentially VSV*ΔG(Luc) replicons, pseudotyped with the amphotropic VSV glycoprotein (VSVg). We used these particles, from here on forward called

Preprints (www.preprints.org) | NOT PEER-REVIEWED | Posted: 5 July 2022 doi:10.20944/preprints202207.0065.v1

VSV*VSVg, to infect VeroE6 cells in presence of increasing concentrations of PDC-109 for two hours, followed by removal of virus-containing supernatent and PDC-109, respectively. A marked and dose-dependent reduction of GFP+ cells was found upon PDC-109 treatment, with overall maximum inhibition levels of up to 75 % (Figure 5A,B). Notably, also delipidated bull SP (dSP) had a similar impact (Figure 5A, B). PDC-109 is derived from dSP, which was included to assess whether antiviral effects are exerted also in the context of complete soluble fractions of ejaculate preparations. Again, cell viabilities were barely affected by either PDC-109 or dSP treatment, which even seemed to slightly increase cell survival at high concentrations (Figure 5C). This phenomenon is likely a result of the protection from VSV*VSVg infections, since this amphotropic pseudotype leads to very strong infections with severe cytopathic effects.

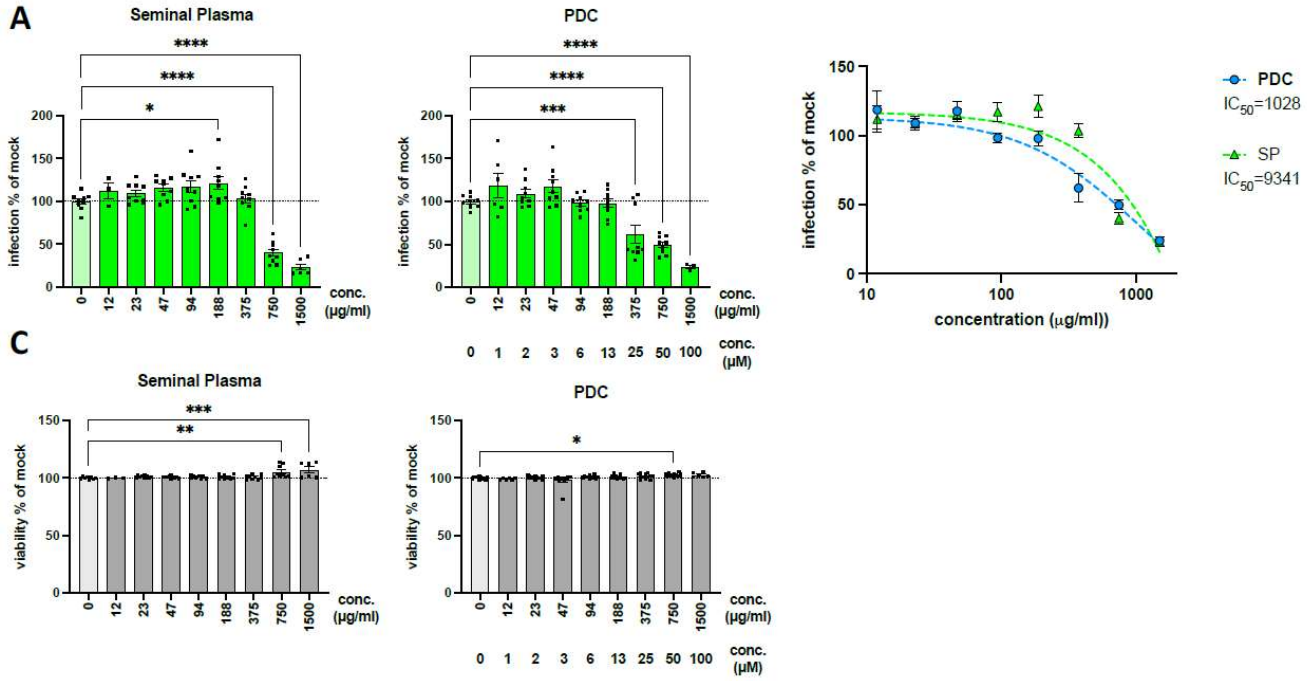

Figure 5: Activity of PDC-109 and SP against VSVg pseudotype infections. (A) The number of GFP+ cells, reflecting the extent of infectivity, was assessed for SP and PDC-109 (PDC) based on flow cytometry measurements. Data were normalized to mock-treated control infections. Bars show mean with SEM. Significance was assesed by parametric one-way analysis of variance (ANOVA) tests, comparing all samples with the mock control (0 µM) and displayed as follows: ****P < 0.0001; ***P < 0.001; **P = 0.001–0.01; *P = 0.01–0.05. Normality of the data was assessed with a Shapiro-Wilk test. **(B)** Inhibitor-response curves were generated using three-parameter fits. IC_{50} values are shown in the legend. **(C)** Viability was assessed by flow cytometry and normalized to mock-treated controls.

Discussion

Bioactive components of mammalian SP exhibit a multitude of functions such as the maintenance of sperm homeostasis or the control of fertilization processes [18,32,33]. In addition, SP has important antimicrobial and antiviral properties, which are so far insufficiently understood. We have recently discovered that the bull SP protein PDC-109 effectively inhibits membrane fusion

 doi:10.20944/preprints202207.0065.v1

between influenza virus and red blood cells [14]. We now extend our study to other viruses to better understand this putative physiological function of PDC-109, which could inform the development of novel bio-inspired and biomimetic drugs.

Many viruses require strict biosafety measures and are often limited to BSL3 facilities, with species-specific approval of experimental procedures by governmental authorities. An attractive alternative are pseudotyped, recombinant reporter viruses, such as the VSV*ΔG(Luc) replicon system, developed by Zimmer and colleagues [34]. Multiple studies have shown that pseudotyped VSV*ΔG(Luc) faithfully replicate the entry-requirements and other pathogen-specific cellular-processes of the wildtype viruses the pseudotyping protein was derived of [35–40]. In the light of the ongoing SARS-CoV-2 pandemic, we first tested whether PDC-109 could have protective effects against VSV* entry, mediated by the SARS-CoV-2 spike protein. In recent months, the VSV*ΔG(Luc) replicon and related systems have been extensively used for SARS-CoV-2 virus entry research, as well as numerous broad-scale neutralization and seroprevalence studies[31,41–45]. Here, we show that PDC-109 completely abolishes VSV*SARS CoV-2 infections at high micromolar concentrations, however accompanied with signficant cytotoxocity when applied for extended periods of time (24 hours, Figure 1). However, if PDC-109 treatment is transiert (limited to 2 h), it permits effective suppression of viral entry with almost no detectable impairment of cellular integrity (Figure 1B, Figure 2). Curiously though, PDC-109 also impacted VSV*SARS CoV-2 infections, when it was added to cells after virus entry (Figure 2), suggesting that VSV* replication too is subject to PDC-109 antiviral activity. Interestingly, pre-treatment and priming with PDC-109 did not protect cells from VSV*SARS CoV-2 infections (Figure 3), suggesting that PDC-109 exerts antiviral effects directly and only when present during viral infections.

We also tested if PDC-109 could alleviate infection burden in live infections with fully infectious SARS-CoV-2 particles (Figure 4). A TCID50 assay was performed to quantify viral infections based on the cytopathic effect of the virus on VeroE6 cells, in presence and absence of increasing concentrations of PDC-109. Again, we found that PDC-109 inhibits viral infections, albeit only to roughly 50% at the maximal concentration, but without any signficant viability effects (Figure S2). As outlined in the results section, our assay likely underestimates the protective effects of PDC-109 since only the first two hours of infection are blocked in treated cells. All secondary infections that occur in the subsequent 70 h of infection are completely PDC-109-independent, which may partly overwrite initial effects of the treatment. In order to circumvent this shortcoming, we performed a complementary experiment in which cells were infected for 24 hours only, thereby effectively abolishing secondary infections. Expectedly, SARS-CoV-2 infections were almost completely suppressed at high PDC-109 concentrations, demonstrating again its strong antiviral effects.

Finally, we have assessed the antiviral activity of PDC-109 against VSV* reporter viruses, pseudotyped with VSVg (Figure 5). VSV utilizes the ubiquitously expressed LDL-receptor (LDL-R) [46] for viral entry, thus enabling VSVg-mediated entry into a broad spectrum of mammalian cell lines and primary cell lineages. In this experiment, we included dSP derived from ejaculates of domestic cattle (*Bos taurus*), containing PDC-109, but also a multitude of other proteins and components, which might either

 doi:10.20944/preprints202207.0065.v1

facilitate or suppress antiviral properties of PDC-109 or even have independent inhibitory effects. Again, PDC-109 significantly and dose-dependly inhibited VSV*VSVg infections of VeroE6 cells and dSP showed a comparable effect, suggesting that PDC-109 is the dominant antiviral factor in SP in our experimental setup. Noteworthily, a recent study has shown strong antiviral effects of human SP against Mumps virus infections and a non-protein component was identified as the bioactive agent [3]. However, to the best of our knowledge, bull SP has hitherto not been thoroughly assessed for antiviral properties, nor have individual factors been identified with protective functions against invading pathogens.

Our results raise the question, how PDC-109 exerts its antiviral activity, but also the cytotoxicity we found upon extented exposure. Previous studies have already shown that PDC-109 is able to lyse human red blood cells, the extent of that depending on the cholesterol content in the erythrocyte membrane. We found a strong decrease of cell viablity when incubating the cells high concentrations of PDC-109 for long time intervals (above 22 h), whereas when treating the cells for 2 h with the protein, cell viability was not significantly influenced. The later result argues against a sole impact of the protein on membrane lipid composition and/or physical-chemical membrane properties as cause of cell lysis (see below) since these modifications should act at the shorter time scale. Therefore, other explanations possibly also considering intracellular effects of PDC-109 have to be taken into account (see also below). However, at the current state, the reasons for the disruption of the cells in the presence of PDC-109 are unknown and will be investigated in future studies.

With regard to the specific molecular mechanisms responsible for the observed antiviral effects, several possibilities seem conceivable. It could be hypothesized that PDC-109 binds to the viral and/or to the plasma membrane (of the target cells) thereby suppressing the attachement of viruses to the cell membrane. Recently, we proposed that such a lipid-binding is mainly responsible for the inhibition of influenza-mediated fusion in the presence of PDC-109 [14]. This mechanism would require that the protein is present during the initial virus-plasma membrane interaction. Indeed, we found that PDC-109 was inhibitory when it was added to cells simultaneously with the virus, but not upon a pre-treatment. An interaction of PDC-109 with viral and/or cell membranes can be explained by its affinity to phosphorylcholine-containing lipids present in either membrane [22]. Alternatively, PDC-109 may also specifically interact with viruses via its Fn II domain. Several studies have shown that infection by many pathogenic bacteria and viruses involves the interaction of their surface protein with the Fn II domain of fibronectin present on the host [52–57].

It is also plausible that PDC-109 influences virus infectivity by more complex mechanisms that would not require the protein to be physically present at the cell-virus-interface. Indeed, our experiments in Calu6 ACE2 cells, in which PDC-109 almost completely abolished infection upon administration after completion of virus entry (Figure 2), indicates effects on virus replication and other intracellular processes. This could suggest that PDC-109 triggers cellular signaling cascades upon binding of cell surface components, which in turn impact viral post-entry steps. Otherwise, PDC-109 may also enter treated cells by endocytosis and then

 doi:10.20944/preprints202207.0065.v1

directly control virus infections intracellularly. Our finding that cytotoxicity of PDC-109 can be prevented by removal of cellular supernatants argues against such large-scale, active internalization of the protein.

Nonetheless, based on a large body of literature we surmise that membrane interactions are critically involved in the antiviral activity of SP and PDC-109. In that context several known effects of the protein have to be considered: (i) incorporation into the membrane bilayer (e.g. influencing membrane curvature and mobility of membrane lipids) [23,24,58,59], (ii) specific interaction with phosphorylcholine-containing lipids and cholesterol (which may modify lateral membrane organization) [22,27,60], and (iii) extraction of phospholipids and preferentially cholesterol from the plasma membrane (e.g. modifying lipid composition) [61,62]. These parameters and properties are known also to be important for the extent of virus infectivity. For instance numerous studies have shown the role of the lipid composition of the target and of the virus membrane, especially the presence and the concentration of cholesterol and sphingolipids [63–65]. For cholesterol, an influence can be mediated by a direct interaction via sterol binding proteins or by its property to form lateral membrane domains [66–68]. Those membrane changes may again indirectly influence membrane proteins which are involved during virus infection [68]. Moreover, the fusion of viruses with target membranes depends on the surface curvature of the participating membranes which is influenced again by cholesterol or by the insertion of peptides/proteins [69–73]. Additionally to these lipid specific effects of PDC-109, also a direct influence on proteins has to be considered based on the described chaperone-like activity [25], i.e. it may interact with proteins which are important for virus replication, e.g. transcription factors, by that exerting an antiviral activity.

Conclusion

Our study has shown, for the first time, significant pan-viral inhibitory effects of the bull SP protein PDC-109 in different cell culture systems and against different viral pseudotypes. PDC-109 potently blocks virus entry and unexpectedly also VSV* virus replication. However, it does not provide lasting protection from viral infections. Upon extended exposure, PDC-109 has significant cytotoxic effects, which can be completely mitigated by early removal and limited application during receptor binding and viral entry only. Our results may represent a novel, interesting direction for the design and development of new antiviral and antibacterial drugs, since SP components from industrial farm animals and livestock are available in large quantities or, in case of proteins, can be recombinantly produced [26] with the aim of a medical application if beneficial effects are identified.

 doi:10.20944/preprints202207.0065.v1

Supplementary Materials

The following supplementary material is provided: Figure S1 (Generation of Calu6 ACE2 cells and SARS CoV-2 pseudotyping.), Figure S2 (Cytotoxicity of PDC-109 in VeroE6 cells.).

Author Contribution

Conceptualization, R.S., K.M. and P.M.; Methodology, P.M. and R.S.; Software, R.S.; Validation, R.S. and P.M.; Formal Analysis, H.S.S.S., R.S. and K.S.; Investigation, H.S.S.S. and K.S.; Resources, R.S., K.M and P.M.; Data Curation, R.S.; Writing – Original Draft Preparation, H.S.S.S., R.S., P.M. and K.M.; Writing – Review & Editing, H.S.S.S., R.S., P.M., K.M and K.S.; Visualization, H.S.S.S. and R.S.; Supervision, R.S., K.M and P.M.; Project Administration, R.S., K.M and P.M.; Funding Acquisition, R.S., K.M and P.M.

Conflicts of Interest

The authors declare no conflict of interest.

Institutional Review Board Statement.

Not applicable.

Informed Consent Statement.

Not applicable.

Data Availability Statement.

Supplementary data are provided. Raw data are available upon request.

Acknowledgements

We thank Ulrike Jakop (IFN Schönow) for her assistance in semen handling and Sabine Schiller (Humboldt University Berlin) for technical assistance. We also thank PD Dr. Gert Zimmer and Drs. Markus Hoffmann and Stefan Pöhlmann for providing the VSV replicon system.

Bibliography

1 Dejucq N & Jégou B (2001) Viruses in the Mammalian Male Genital Tract and Their Effects on the Reproductive System. *Microbiol Mol Biol Rev* **65**, 208–231.

2 Lippold S, Braun B, Krüger F, Harms M, Müller JA, Groß R, Münch J & von Einem J (2019) Natural Inhibitor of Human Cytomegalovirus in Human Seminal Plasma. *J Virol* **93**.

3 Chen R, Zhang W, Gong M, Wang F, Wu H, Liu W, Gao Y, Liu B, Chen S, Lu W, Yu X, Liu A, Han R, Chen Y & Han D (2021) Characterization of an Antiviral Component in Human Seminal Plasma. *Front Immunol* **12**.

4 Münch J, Rücker E, Ständker L, Adermann K, Goffinet C, Schindler M, Wildum S, Chinnadurai R, Rajan D, Specht A, Giménez-Gallego G, Sánchez PC, Fowler DM, Koulov A, Kelly JW, Mothes W, Grivel JC, Margolis L, Keppler OT, Forssmann WG, Kirchhoff F, Munch J, Rucker E, Standker L, Adermann K, Goffinet C, Schindler M, Wildum S, Chinnadurai R, Rajan D, Specht A, Gimenez-Gallego G, Sanchez PC, Fowler DM, Koulov A, Kelly JW, Mothes W, Grivel JC, Margolis L, Keppler OT, Forssmann WG & Kirchhoff F (2007) Semen-derived amyloid fibrils drastically enhance HIV infection. *Cell* **131**, 1059–1071.

5 Bouvet J-P, Grésenguet G & Bélec L (1997) Vaginal pH neutralization by semen as a cofactor of HIV transmission. *Clin Microbiol Infect* **3**, 19–23.

6 Nijmeijer BM, Bermejo-Jambrina M, Kaptein TM, Ribeiro CMS, Wilflingseder D & Geijtenbeek TBH (2021) HIV-1 subverts the complement system in semen to enhance viral transmission. *Mucosal Immunol* **14**, 743–750.

7 Martellini JA, Cole AL, Venkataraman N, Quinn GA, Svoboda P, Gangrade BK, Pohl J, Sørensen OE & Cole AM (2009) Cationic polypeptides contribute to the anti-HIV-1 activity of human seminal plasma. *FASEB J* **23**, 3609–3618.

8 Malm J, Sørensen O, Persson T, Frohm-Nilsson M, Johansson B, Bjartell A, Lilja H, Ståhle-Bäckdahl M, Borregaard N & Egesten A (2000) The Human Cationic Antimicrobial Protein (hCAP-18) Is Expressed in the Epithelium of Human Epididymis, Is Present in Seminal Plasma at High Concentrations, and Is Attached to Spermatozoa. *Infect Immun* **68**, 4297–4302.

9 Doncel GF, Joseph T & Thurman AR (2011) Role of Semen in HIV-1 Transmission: Inhibitor or facilitator? *Am J Reprod Immunol* **65**, 292–301.

10 Christopher-Hennings J, Nelson EA, Althouse GC & Lunney J (2008) Comparative antiviral and proviral factors in semen and vaccines for preventing viral dissemination from the male reproductive tract and semen. *Anim Heal Res Rev* **9**, 59–69.

11 Sabatte J, Faigle W, Ceballos A, Morelle W, Rodríguez Rodrígues C, Remes Lenicov F, Thépaut M, Fieschi F, Malchiodi E, Fernández M, Arenzana-Seisdedos F, Lortat-Jacob H, Michalski J-C, Geffner J & Amigorena S (2011) Semen Clusterin Is a Novel DC-SIGN Ligand. *J Immunol* **187**, 5299–5309.

12 Kim K-A, Yolamanova M, Zirafi O, Roan NR, Standker L, Forssmann W-G, Burgener A, Dejucq-Rainsford N, Hahn BH, Shaw GM, Greene WC, Kirchhoff F & Muench J (2010) Semen-mediated enhancement of HIV infection is donor-dependent and correlates with the levels of SEVI. *Retrovirology* **7**, 55.

13 Madison MN, Roller RJ & Okeoma CM (2014) Human semen contains exosomes with potent anti-HIV-1 activity. *Retrovirology* **11**, 102.

14 Welke RW, Haralampiev I, Schröter F, Braun BC, Herrmann A, Sieben C & Müller P (2019) Inhibition of influenza virus activity by the bovine seminal plasma protein PDC-109. *Eur Biophys J* **48**, 503–511.

15 Fan J, Lefebvre J & Manjunath P (2006) Bovine seminal plasma proteins and their relatives: A new expanding superfamily in mammals. *Gene* **375**, 63–74.

16 Calvete JJ & Sanz L (2007) Insights into structure-function correlations of ungulate seminal plasma proteins. *Soc Reprod Fertil Suppl* **65**, 201–15.
17 Ekhlasi-Hundrieser M., Müller P. and T-PE (209AD) Male secretory proteins sperm tools for fertilisation. In *Biology of male germ cells* pp. 173–210. Shaker Publisher GmbH.
18 Rodríguez-Martínez H, Kvist U, Ernerudh J, Sanz L & Calvete JJ (2011) Seminal Plasma Proteins: What Role Do They Play? *Am J Reprod Immunol* **66**, 11–22.
19 Caballero I, Parrilla I, Almiñana C, del Olmo D, Roca J, Martínez E & Vázquez J (2012) Seminal Plasma Proteins as Modulators of the Sperm Function and Their Application in Sperm Biotechnologies. *Reprod Domest Anim* **47**, 12–21.
20 Gwathmey TM, Ignotz GG, Mueller JL, Manjunath P & Suarez SS (2006) Bovine Seminal Plasma Proteins PDC-109, BSP-A3, and BSP-30-kDa Share Functional Roles in Storing Sperm in the Oviduct1. *Biol Reprod* **75**, 501–507.
21 Gasset M, Magdaleno L & Calvete JJ (2000) Biophysical Study of the Perturbation of Model Membrane Structure Caused by Seminal Plasma Protein PDC-109. *Arch Biochem Biophys* **374**, 241–247.
22 Desnoyers L & Manjunath P (1992) Major proteins of bovine seminal plasma exhibit novel interactions with phospholipid. *J Biol Chem* **267**, 10149–55.
23 Ramakrishnan M, Anbazhagan V, Pratap TV, Marsh D & Swamy MJ (2001) Membrane Insertion and Lipid-Protein Interactions of Bovine Seminal Plasma Protein PDC-109 Investigated by Spin-Label Electron Spin Resonance Spectroscopy. *Biophys J* **81**, 2215–2225.
24 Greube A, Müller K, Töpfer-Petersen E, Herrmann A & Müller P (2001) Influence of the bovine seminal plasma protein PDC-109 on the physical state of membranes. *Biochemistry* **40**, 8326–34.
25 Sankhala RS & Swamy MJ (2010) The Major Protein of Bovine Seminal Plasma, PDC-109, Is a Molecular Chaperone. *Biochemistry* **49**, 3908–3918.
26 Calvete JJ, Varela PF, Sanz L, Romero A, Mann K & Töpfer-Petersen E (1996) A Procedure for the Large-Scale Isolation of Major Bovine Seminal Plasma Proteins. *Protein Expr Purif* **8**, 48–56.
27 Leblond E, Desnoyers L & Manjunath P (1993) Phosphorylcholine-binding proteins from the seminal fluids of different species share antigenic determinants with the major proteins of bovine seminal plasma. *Mol Reprod Dev* **34**, 443–449.
28 Roost HP, Bachmann MF, Haag A, Kalinke U, Pliska V, Hengartner H & Zinkernagel RM (1995) Early high-affinity neutralizing anti-viral IgG responses without further overall improvements of affinity. *Proc Natl Acad Sci* **92**, 1257–1261.
29 Heilingloh CS, Aufderhorst UW, Schipper L, Dittmer U, Witzke O, Yang D, Zheng X, Sutter K, Trilling M, Alt M, Steinmann E & Krawczyk A (2020) Susceptibility of SARS-CoV-2 to UV irradiation. *Am J Infect Control* **48**, 1273–1275.
30 Schöler L, Le-Trilling VTK, Eilbrecht M, Mennerich D, Anastasiou OE, Krawczyk A, Herrmann A, Dittmer U & Trilling M (2020) A Novel In-Cell ELISA Assay Allows Rapid and Automated Quantification of SARS-CoV-2 to Analyze Neutralizing Antibodies and Antiviral Compounds. *Front Immunol* **11**.
31 Hoffmann M, Kleine-Weber H, Schroeder S, Mü MA, Drosten C, Pö S, Krü N, Herrler T, Erichsen S, Schiergens TS, Herrler G, Wu N-H, Nitsche A & Pö Hlmann S (2020) SARS-CoV-2 Cell Entry Depends on ACE2 and TMPRSS2 and Is Blocked by a Clinically Proven Protease Inhibitor Article SARS-CoV-2 Cell Entry Depends on ACE2 and TMPRSS2 and Is Blocked by a Clinically Proven Protease Inhibitor. *Cell* **181**, 1–10.
32 Manjunath P, Bergeron A, Lefebvre J & Fan J (2007) Seminal plasma proteins: functions and interaction with protective agents during semen preservation. *Soc Reprod Fertil Suppl* **65**, 217–28.
33 Bedford JM (2015) The Functions—or Not—of Seminal Plasma? *Biol Reprod* **92**.
34 Berger Rentsch M & Zimmer G (2011) A Vesicular Stomatitis Virus Replicon-Based Bioassay for the Rapid and Sensitive Determination of Multi-Species Type I Interferon. *PLoS One* **6**, e25858.
35 Carette JE, Raaben M, Wong AC, Herbert AS, Obernosterer G, Mulherkar N, Kuehne AI, Kranzusch PJ, Griffin AM, Ruthel G, Cin PD, Dye JM, Whelan SP, Chandran K & Brummelkamp TR (2011) Ebola virus entry requires the cholesterol transporter Niemann–Pick C1. *Nature* **477**, 340–343.
36 Jae LT, Raaben M, Herbert a. S, Kuehne a. I, Wirchnianski a. S, Soh TK, Stubbs SH, Janssen H, Damme M, Saftig P, Whelan SP, Dye JM & Brummelkamp TR (2014) Lassa virus entry requires a trigger-induced receptor switch. *Science (80-)* **344**, 1506–1510.
37 Jangra RK, Herbert AS, Li R, Jae LT, Kleinfelter LM, Slough MM, Barker SL, Guardado-Calvo P, Román-Sosa G, Dieterle ME, Kuehne AI, Muena NA, Wirchnianski AS, Nyakatura EK, Fels JM, Ng M, Mittler E, Pan J, Bharrhan S, Wec AZ, Lai JR, Sidhu SS, Tischler ND, Rey FA, Moffat J, Brummelkamp TR, Wang Z, Dye JM & Chandran K (2018) Protocadherin-1 is essential for cell entry by New World hantaviruses. *Nature* **563**, 559–563.
38 Kondratowicz AS, Lennemann NJ, Sinn PL, Davey RA, Hunt CL, Moller-Tank S, Meyerholz DK, Rennert P, Mullins RF, Brindley M, Sandersfeld LM, Quinn K, Weller M, McCray Jr. PB, Chiorini J & Maury W (2011) T-cell immunoglobulin and mucin domain

1 (TIM-1) is a receptor for Zaire Ebolavirus and Lake Victoria Marburgvirus. *Proc Natl Acad Sci U S A* **108**, 8426–8431.

39 Raaben M, Jae LT, Herbert AS, Kuehne AI, Stubbs SH, Chou Y, Blomen VA, Kirchhausen T, Dye JM, Brummelkamp TR & Whelan SP (2017) NRP2 and CD63 Are Host Factors for Lujo Virus Cell Entry. *Cell Host Microbe* **22**, 688-696.e5.

40 Riblett AM, Blomen VA, Jae LT, Altamura LA, Doms RW, Brummelkamp TR & Wojcechowskyj JA (2016) A Haploid Genetic Screen Identifies Heparan Sulfate Proteoglycans Supporting Rift Valley Fever Virus Infection. *J Virol* **90**, 1414–1423.

41 Salazar-García M, Acosta-Contreras S, Rodríguez-Martínez G, Cruz-Rangel A, Flores-Alanis A, Patiño-López G & Luna-Pineda VM (2022) Pseudotyped Vesicular Stomatitis Virus-Severe Acute Respiratory Syndrome-Coronavirus-2 Spike for the Study of Variants, Vaccines, and Therapeutics Against Coronavirus Disease 2019. *Front Microbiol* **12**.

42 Ng DL, Goldgof GM, Shy BR, Levine AG, Balcerek J, Bapat SP, Prostko J, Rodgers M, Coller K, Pearce S, Franz S, Du L, Stone M, Pillai SK, Sotomayor-Gonzalez A, Servellita V, Martin CSS, Granados A, Glasner DR, Han LM, Truong K, Akagi N, Nguyen DN, Neumann NM, Qazi D, Hsu E, Gu W, Santos YA, Custer B, Green V, Williamson P, Hills NK, Lu CM, Whitman JD, Stramer SL, Wang C, Reyes K, Hakim JMC, Sujishi K, Alazzeh F, Pham L, Thornborrow E, Oon C-Y, Miller S, Kurtz T, Simmons G, Hackett J, Busch MP & Chiu CY (2020) SARS-CoV-2 seroprevalence and neutralizing activity in donor and patient blood. *Nat Commun* **11**, 4698.

43 Oguntuyo KY, Stevens CS, Hung CT, Ikegame S, Acklin JA, Kowdle SS, Carmichael JC, Chiu H-P, Azarm KD, Haas GD, Amanat F, Klingler J, Baine I, Arinsburg S, Bandres JC, Siddiquey MNA, Schilke RM, Woolard MD, Zhang H, Duty AJ, Kraus TA, Moran TM, Tortorella D, Lim JK, Gamarnik A V., Hioe CE, Zolla-Pazner S, Ivanov SS, Kamil JP, Krammer F & Lee B (2021) Quantifying Absolute Neutralization Titers against SARS-CoV-2 by a Standardized Virus Neutralization Assay Allows for Cross-Cohort Comparisons of COVID-19 Sera. *MBio* **12**.

44 Borena W, Bánki Z, Bates K, Winner H, Riepler L, Rössler A, Pipperger L, Theurl I, Falkensammer B, Ulmer H, Walser A, Pichler D, Baumgartner M, Schönherr S, Forer L, Knabl L, Würzner R, von Laer D, Paetzold J & Kimpel J (2021) Persistence of immunity to SARS-CoV-2 over time in the ski resort Ischgl. *EBioMedicine* **70**, 103534.

45 Lu Y, Wang J, Li Q, Hu H, Lu J & Chen Z (2021) Advances in Neutralization Assays for SARS-CoV-2. *Scand J Immunol* **94**.

46 Finkelshtein D, Werman A, Novick D, Barak S & Rubinstein M (2013) LDL receptor and its family members serve as the cellular receptors for vesicular stomatitis virus. *Proc Natl Acad Sci* **110**, 7306–7311.

47 Roelofsen B, Meer G Van & Opdenkamp JAF (1981) The lipids of red cell membranes: Compositional, structural and functional aspects. *Scand J Clin Lab Invest* **41**, 111–115.

48 Singh BP, Asthana A, Basu A, Tangirala R, Mohan Rao C & Swamy MJ (2020) Conserved core tryptophans of FnII domains are crucial for the membranolytic and chaperone-like activities of bovine seminal plasma protein PDC-109. *FEBS Lett* **594**, 509–518.

49 Tannert A, Töpfer-Petersen E, Herrmann A, Müller K & Müller P (2007) The Lipid Composition Modulates the Influence of the Bovine Seminal Plasma Protein PDC-109 on Membrane Stability. *Biochemistry* **46**, 11621–11629.

50 Parks JE & Lynch D V. (1992) Lipid composition and thermotropic phase behavior of boar, bull, stallion, and rooster sperm membranes. *Cryobiology* **29**, 255–266.

51 Meer G Van, Voelker D & Feigenson G (2008) Membrane lipids - where they are and how they behave.pdf. *Nat Rev Mol …* **9**, 112–124.

52 De Petro G, Barlati S, Vartio T & Vaheri A (1981) Transformation-enhancing activity of gelatin-binding fragments of fibronectin. *Proc Natl Acad Sci* **78**, 4965–4969.

53 Atkin KE, Brentnall AS, Harris G, Bingham RJ, Erat MC, Millard CJ, Schwarz-Linek U, Staunton D, Vakonakis I, Campbell ID & Potts JR (2010) The Streptococcal Binding Site in the Gelatin-binding Domain of Fibronectin Is Consistent with a Non-linear Arrangement of Modules. *J Biol Chem* **285**, 36977–36983.

54 Larson CL, Samuelson DR, Eucker TP, O'Loughlin JL & Konkel ME (2013) The fibronectin-binding motif within FlpA facilitates Campylobacter jejuni adherence to host cell and activation of host cell signaling. *Emerg Microbes Infect* **2**, 1–12.

55 Kobayashi K & Koike S (2020) Cellular receptors for enterovirus A71. *J Biomed Sci* **27**, 23.

56 Keski-Oja J, Hautanen A & Julkunen I (1987) Fibronectin and Viral Pathogenesis. *Clin Infect Dis* **9**, S404–S411.

57 Pande H, Terramani T, Tressel T, Churchill MA, Hawkins GG & Zaia JA (1990) Altered expression of fibronectin gene in cells infected with human cytomegalovirus. *J Virol* **64**, 1366–1369.

58 Müller P, Erlemann K-R, Müller K, Calvete JJ, Töpfer-Petersen E, Marienfeld K & Herrmann A (1998) Biophysical characterization of the interaction of bovine seminal plasma protein PDC-109 with phospholipid vesicles. *Eur Biophys J* **27**, 33–41.

59 Le Guillou J, Ropers M-H, Gaillard C, David-Briand E, van Leeuwen-Ibarrola J, Desherces S, Schmitt E, Bencharif D, Amirat-Briand L, Anton M & Tainturier D (2016) Sequestration of bovine seminal plasma proteins by different assemblies of phosphatidylcholine: A new technical approach. *Colloids Surfaces B Biointerfaces* **140**, 523–530.

60 Müller P, Greube A, Töpfer-Petersen E & Herrmann A (2002) Influence of the bovine seminal plasma protein PDC-109 on

cholesterol in the presence of phospholipids. *Eur Biophys J* **31**, 438–447.

61 Moreau R, Frank PG, Perreault C, Marcel YL & Manjunath P (1999) Seminal plasma choline phospholipid-binding proteins stimulate cellular cholesterol and phospholipid efflux. *Biochim Biophys Acta - Mol Cell Biol Lipids* **1438**, 38–46.

62 Moreau R, Thérien I, Lazure C & Manjunath P (1998) Type II Domains of BSP-A1/-A2 Proteins: Binding Properties, Lipid Efflux, and Sperm Capacitation Potential. *Biochem Biophys Res Commun* **246**, 148–154.

63 Dumas F, Preira P & Salomé L (2014) Membrane organization of virus and target cell plays a role in HIV entry. *Biochimie* **107**, 22–27.

64 Raulin J (2000) Lipids and retroviruses. *Lipids* **35**, 123–130.

65 Kočar E, Režen T & Rozman D (2021) Cholesterol, lipoproteins, and COVID-19: Basic concepts and clinical applications. *Biochim Biophys Acta - Mol Cell Biol Lipids* **1866**, 158849.

66 Molotkovsky R, Alexandrova V, Galimzyanov T, Jiménez-Munguía I, Pavlov K, Batishchev O & Akimov S (2018) Lateral Membrane Heterogeneity Regulates Viral-Induced Membrane Fusion during HIV Entry. *Int J Mol Sci* **19**, 1483.

67 Fantini J, Epand RM & Barrantes FJ (2019) Cholesterol-Recognition Motifs in Membrane Proteins. In pp. 3–25.

68 Campbell SM, Crowe SM & Mak J (2001) Lipid rafts and HIV-1: From viral entry to assembly of progeny virions. In *Journal of Clinical Virology* pp. 217–227.

69 Ivankin A, Kuzmenko I & Gidalevitz D (2012) Cholesterol Mediates Membrane Curvature during Fusion Events. *Phys Rev Lett* **108**, 238103.

70 Razinkov VI, Melikyan GB, Epand RM, Epand RF & Cohen FS (1998) Effects of Spontaneous Bilayer Curvature on Influenza Virus–mediated Fusion Pores. *J Gen Physiol* **112**, 409–422.

71 Stiasny K & Heinz FX (2004) Effect of Membrane Curvature-Modifying Lipids on Membrane Fusion by Tick-Borne Encephalitis Virus. *J Virol* **78**, 8536–8542.

72 Inamdar K, Tsai F-C, Dibsy R, de Poret A, Manzi J, Merida P, Muller R, Lappalainen P, Roingeard P, Mak J, Bassereau P, Favard C & Muriaux D (2021) Full assembly of HIV-1 particles requires assistance of the membrane curvature factor IRSp53. *Elife* **10**.

73 Grover JR, Llewellyn GN, Soheilian F, Nagashima K, Veatch SL & Ono A (2013) Roles played by capsid-dependent induction of membrane curvature and Gag-ESCRT interactions in tetherin recruitment to HIV-1 assembly sites. *J Virol* **87**, 4650–4664.